9306 *Biochemistry* **2009,** *48,* 9306–9312
DOI: 10.1021/bi900956p

BIOCHEMISTRY
including biophysical chemistry & molecular biology
Article

Role of the Carbonyl Group of the (6−4) Photoproduct in the (6−4) Photolyase Reaction[†]

Junpei Yamamoto,[‡] Kenichi Hitomi,[‡,§] Ryosuke Hayashi,[‡] Elizabeth D. Getzoff,[§] and Shigenori Iwai*[,‡]

[‡]*Division of Chemistry, Graduate School of Engineering Science, Osaka University, 1-3 Machikaneyama, Toyonaka, Osaka 560-8531, Japan, and* [§]*Department of Molecular Biology and The Skaggs Institute for Chemical Biology, The Scripps Research Institute, La Jolla, California 92037*

Received June 6, 2009; Revised Manuscript Received August 11, 2009

ABSTRACT: The (6−4) photoproduct, which is one of the major UV-induced DNA lesions, causes carcinogenesis with high frequency. The (6−4) photolyase is a flavoprotein that can restore this lesion to the original bases, but its repair mechanism has not been elucidated. In this study, we focused on the interaction between the enzyme and the 3′ pyrimidone component of the (6−4) photoproduct and prepared a substrate analogue in which the carbonyl group, a hydrogen-bond acceptor, was replaced with an imine, a hydrogen-bond donor, to investigate the involvement of this carbonyl group in the (6−4) photolyase reaction. UV irradiation of oligodeoxyribonucleotides containing a single thymine−5-methylisocytosine site yielded products with absorption bands at wavelengths longer than 300 nm, similar to those obtained from the conversion of the TT site to the (6−4) photoproduct. Nuclease digestion, MALDI-TOF mass spectrometry, and the instability of the products indicated the formation of the 2-iminopyrimidine-type photoproduct. Analyses of the reaction and the binding of the (6−4) photolyase using these oligonucleotides revealed that this imine analogue of the (6−4) photoproduct was not repaired by the (6−4) photolyase, although the enzyme bound to the oligonucleotide with considerable affinity. These results indicate that the carbonyl group of the 3′ pyrimidone ring plays an important role in the (6−4) photolyase reaction. On the basis of these results, we discuss the repair mechanism.

The base moieties within DNA are excited by exposure to ultraviolet (UV)[1] light and undergo various chemical reactions that alter their structures. The major products of these reactions are cyclobutane pyrimidine dimers (CPDs) and pyrimidine-(6−4)pyrimidone photoproducts [(6−4) photoproducts **1**] (*1*). The simplest repair pathway for these UV lesions involves photoreactivation of the UV-damaged DNA, which uses blue to near-UV light (300−500 nm) in sunlight to maintain genetic integrity (*2*, *3*). The CPD and (6−4) photolyases are the enzymes responsible for the photoreactivation of the CPD and the (6−4) photoproduct, respectively. These enzymes share sequence similarity and contain the same cofactor, flavin adenine dinucleotide (FAD), in their catalytic centers. However, their repair processes are remarkably different (*2*). While the CPD is repaired by donation of an electron from the excited $FADH^-$ cofactor to the cyclobutane ring (*4*, *5*), the repair of the (6−4) photoproduct requires not only the light-driven electron transfer but also the migration of the functional group from C5 of the 5′ base to C4 of the 3′ pyrimidone.

It has been proposed that the migration of the functional group within the (6−4) photoproduct could be accomplished by the formation of the oxetane/azetidine intermediate (*6*), catalyzed by the two conserved histidine residues of the (6−4) photolyase (Figure 1A) (*7*). An electron−nuclear double resonance analysis suggested that one of these histidine residues that could act as an acid was protonated at pH 9.5 in *Xenopus laevis* (6−4) photolyase. In the proposed repair mechanism, this protonated histidine interacts with N3 of the pyrimidone of the (6−4) photoproduct, and the other histidine interacts with the 5-OH group of the 5′ component (*8*). The oxetane-mediated pathway was shown to be necessary for the light-dependent repair of the (6−4) photoproduct in biochemical studies (*9*, *10*), model compound chemistry analyses (*11*, *12*), and quantum calculations (*13*). In the crystal structure of the *Drosophila melanogaster* (6−4) photolyase−DNA complex (*14*), however, the enzyme interacted only with the 5-OH group of the 5′ base of the (6−4) photoproduct. Therefore, on the basis of this structure and the in situ repair in the crystal, a different reaction mechanism has been proposed; the functional group in question was directly transferred to C4 of the 3′ base, without oxetane intermediate formation (Figure 1B).

Although an interaction was not detected between the enzyme and the 3′ pyrimidone in the *D. melanogaster* (6−4) photolyase−DNA complex structure, the 3′ pyrimidone may still be involved in the (6−4) photolyase reaction. In our previous study using the Dewar photoproduct, we discovered that the 3′ component of the (6−4) photoproduct was important for substrate recognition by the (6−4) photolyase (*15*). This result suggested that the active site of the (6−4) photolyase could interact with the 3′ pyrimidone of the (6−4) photoproduct. In the originally proposed mechanism (*6*, *7*), N3 of the 3′ pyrimidone was chosen as a hydrogen-bond acceptor, probably because this atom was close to the donor. However, the 3′ pyrimidone contains two hydrogen-bond

[†]This research was supported by a Grant-in-Aid for JSPS Fellows (20·1148 to J.Y.) from the Ministry of Education, Culture, Sports, Science, and Technology, Japan; The Skaggs Institute for Chemical Biology (K.H.); and a National Institutes of Health Grant (GM37684 to E.D.G.).

*To whom correspondence should be addressed. Telephone: +81-6-6850-6250. Fax: +81-6-6850-6240. E-mail: iwai@chem.es.osaka-u.ac.jp.

[1]Abbreviations: UV, ultraviolet; CPD, cyclobutane pyrimidine dimer; (6−4) photoproduct, pyrimidine(6−4)pyrimidone photoproduct; FAD, flavin adenine dinucleotide; HPLC, high-performance liquid chromatography; TEAA, triethylammonium acetate; 3-HPA, 3-hydroxypicolinic acid; MALDI-TOF MS, matrix-assisted laser desorption ionization time-of-flight mass spectrometry; EMSA, electrophoretic mobility shift assay; dmisoC, 2′-deoxy-5-methylisocytidine; $T(6-4)T^{NH2}$, (6−4) photoproduct in which the carbonyl group is substituted with an imine; T(6−4)T, (6−4) photoproduct formed at the TT site; TpdmisoC, thymidylyl(3′−5′)-2′-deoxy-5-methylisocytidine; t_R, retention time; FAB, fast atom bombardment.

 Published on Web 08/28/2009

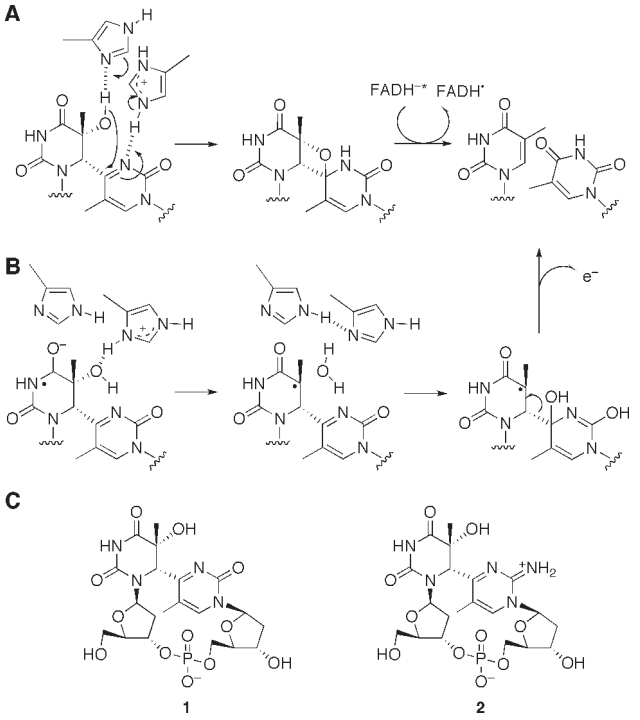

FIGURE 1: Repair mechanisms of the (6−4) photolyase proposed from site-directed mutagenesis (A) and crystallographic analysis (B). The first radical anion species in panel B was derived from light-dependent electron transfer. (C) Structures of the (6−4) photoproduct formed at the TT site [T(6−4)T, **1**] and the cationic imine analogue of the (6−4) photoproduct [$T(6-4)T^{NH2}$, **2**] used in this study.

acceptors, namely, the N3 atom and the C2 carbonyl group. Our study with the dinucleoside monophosphate containing the (6−4) photoproduct showed an extremely low pK_a for N3 of the 3′ pyrimidone of the (6−4) photoproduct, compared with that of the normal pyrimidone ring, and suggested formation of an intramolecular hydrogen bond between N3 of the 3′ base and the 5-OH group of the 5′ base (*16*). Therefore, the possible involvement of the C2 carbonyl, rather than N3, of the 3′ pyrimidone in the reaction should be considered. To investigate this possibility, the photolyase reaction with a substrate analogue modified at this functional group would provide useful information. Previously, a thietane-type photoproduct and its derivatives were used as substrate analogues for the (6−4) photolyase reaction (*9*), but the use of compounds modified at the C2 position has not been reported thus far.

In this article, we investigated the role of the C2 carbonyl group of the 3′ pyrimidone in photoproduct repair by (6−4) photolyase, by preparing oligodeoxyribonucleotides containing a modified (6−4) photoproduct [$T(6-4)T^{NH2}$, **2**], in which this carbonyl group was replaced with an iminium cation. The results of the reaction and the binding experiments using this modified substrate indicate that the carbonyl group at the 3′ pyrimidone of the (6−4) photoproduct is involved in the repair of the (6−4) photoproduct by the (6−4) photolyase. We further discuss the role of this carbonyl group in the reaction mechanism of the (6−4) photolyase.

MATERIALS AND METHODS

General Methods. Reagents for the DNA synthesizer were purchased from Applied Biosystems Japan and Glen Research. HPLC analyses were performed on either a Gilson gradient-type analytical system equipped with a Waters 2996 photodiode array detector or a Shimadzu gradient-type analytical system equipped with an SPD-M10AVP photodiode array detector. On both systems, a Waters μBondasphere C18, 5 μm, 300 Å column (3.9 mm × 150 mm) was used at a flow rate of 1.0 mL/min with a linear gradient of acetonitrile (Wako Pure Chemical Co. Ltd.) in 0.1 M triethylammonium acetate (TEAA) (pH 7.0). ^{1}H NMR spectra were recorded on a Varian INOVA 500 spectrometer at 303 K. An HDO signal in D_2O was set to 4.70 ppm as an internal reference. The mixing time in the NOESY measurement was set to 700 ms. Analysis of oligonucleotides by matrix-assisted laser desorption ionization time-of-flight mass spectrometry (MALDI-TOF MS) was performed on an Applied Biosystems Voyager DE PRO spectrometer, using 3-hydroxypicolinic acid (3-HPA) as a matrix. The competitive electrophoretic mobility shift assay (EMSA) was performed in a cold room maintained at 4−6 °C under yellow light, to prevent the repair reaction by the (6−4) photolyase. The results of the radioisotope experiments were obtained with a BAS-1800 Bioimaging Analyzer (Fuji Film).

Preparation, Purification, and Characterization of the Oligonucleotides Containing the (6−4) Photoproduct Analogue. Oligonucleotides containing 2′-deoxy-5-methylisocytidine (dmisoC), namely, the dmisoC 12-mer [d(CATmisoCAGCACG-AC)] and the dmisoC 15-mer [d(ACAGCGGTmisoCGCAG-GT)], were synthesized on an Applied Biosystems 3400 DNA synthesizer according to the instructions for the dmf-protected dmisoC phosphoramidite (Glen Research). The oligonucleotides were purified by HPLC. The column was heated to 50 °C, and the elution was performed with a 5 to 13% acetonitrile gradient generated over 20 min. Desalting was accomplished with an illustra NAP-10 column (GE Healthcare).

For small-scale tests, oligonucleotides (10 nmol) were dissolved in 1 mL of 50 mM phosphate buffer (pH 7.0). After being degassed by a nitrogen purge for 3 min, the solution was placed in a Petri dish (2.5 cm diameter) and irradiated on ice with a FUNA-UV cross-linker FS-1500 (Funakoshi) with six 15 W germicidal lamps. Aliquots of the solution (20 μL each) were analyzed by HPLC at appropriate intervals. For large-scale preparation, oligonucleotides (100 nmol) were dissolved in 10 mL of 50 mM phosphate buffer (pH 7.0). The solution was degassed for 5 min and then placed in a Petri dish (9.4 cm diameter). The solutions of the 12- and 15-mer were irradiated on ice for 10 and 45 min, respectively. The resulting solution was evaporated to dryness on a rotary evaporator equipped with a vacuum pump, without heating. The residue was dissolved in 1 mL of water, and the oligonucleotides were purified by HPLC. The collected fraction was immediately frozen, to prevent decomposition. After evaporation of the acetonitrile, the solution was passed through a Waters Sep-Pak Plus C18 Environmental Cartridge (Waters) to remove the TEAA. The cartridge was washed with water (10 mL), and then the product was eluted with 50% aqueous acetonitrile (15 mL). The solution was concentrated to dryness, and the residue was dissolved in 400 μL of cold water.

Oligonucleotides containing the normal (6−4) photoproduct [T(6−4)T], d(CATTAGCACGAC) and d(ACAGCGGTTGC-AGGT), where the underlined TT represents the (6−4) photoproduct formed at the TT site, were prepared as described previously (*14*, *17*).

For the nuclease digestion of the oligonucleotide, 150−180 units of S1 nuclease from *Aspergillus oryzae* (Takara Bio) was added to a solution of the oligonucleotide (300 pmol), in a buffer (20 μL) containing 30 mM sodium acetate (pH 4.6), 280 mM NaCl, and 1 mM $ZnSO_4$, and the resultant mixture was incubated at 37 °C for

24 h. Then, 1 unit of alkaline phosphatase from *Escherichia coli* (Takara Bio) and a buffer containing 50 mM Tris-HCl and 1 mM $MgSO_4$ (pH 9.0, 50 μL) were added, and the mixture was incubated for 2 h. The HPLC analysis was performed using a GL Science Inertsil ODS-2 column (4.6 mm × 150 mm) with a linear gradient (from 0 to 10%) of acetonitrile in 0.1 M TEAA for 20 min at room temperature.

Analysis of the (6−4) Photolyase Reaction by HPLC. X. laevis (6−4) photolyase was prepared as described previously (*10*). Analysis of the (6−4) photolyase reaction was performed by HPLC, following our previous report (*15*). Briefly, a solution of *X. laevis* (6−4) photolyase (1 nmol) in a buffer containing 10 mM Tris-HCl (pH 8.0), 10 mM NaCl, and 2 mM 2-mercaptoethanol, which was covered with a Pyrex lid, was illuminated on ice with an 18 W fluorescent lamp at a distance of 15 cm for 30 min. A solution of T(6−4)T 12-mer or $T(6-4)T^{NH2}$ 12-mer (each 200 pmol) was added to the preincubated mixture, and the mixture was illuminated again for 3 h. The reaction mixture was analyzed by HPLC. A linear gradient from 7 to 13% acetonitrile in 0.1 M TEAA generated over 20 min was used for this analysis at room temperature.

Analyses of (6−4) Photolyase Binding by an Electrophoretic Mobility Shift Assay (EMSA). The 5′ end of the T(6−4)T 15-mer (5 pmol) was ^{32}P-labeled with [γ-^{32}P]ATP and T4 polynucleotide kinase. The resultant reaction mixture was passed through an illustra MicroSpin G-25 column (GE Healthcare). The labeled oligonucleotide (250 fmol) was annealed to the unlabeled complementary strand, d(ACCTGCAACCGCTGT) (300 fmol), in a buffer (50 μL) containing 50 mM Tris-HCl (pH 8.0) and 50 mM NaCl. For the competitive EMSA, 0.5 nM [^{32}P]T(6−4)T 15 bp and 50 nM *Xenopus* (6−4) photolyase were mixed in a buffer (20 μL) containing 10 mM Tris-HCl (pH 8.0), 10 mM NaCl, 1 mM DTT, and 5% glycerol, and this mixture was incubated for 10 min. The unlabeled 15 bp duplex containing T(6−4)T, $T(6-4)T^{NH2}$, or undamaged TT was then added to the preincubated mixture, at final concentrations of 0−500 nM. The resultant mixture was incubated for 30 min and then subjected to electrophoresis on a 5% polyacrylamide gel. The band intensity was quantified with Multi Gauge version 3.0 data processing software (Fuji Film). The inhibition constants (K_i) were determined from a Scatchard plot, as described in the Supporting Information.

RESULTS

Preparation and Characterization of Oligonucleotides Containing the (6−4) Photoproduct Analogue. At first, we tried to prepare a 2-thio-modified (6−4) photoproduct, in which the carbonyl group at C2 of the 3′ pyrimidone was replaced with a thiocarbonyl group, and tested whether the (6−4) photoproduct could be formed from thymidylyl(3′−5′)-2-thiothymidine by exposure to UV light. However, we could not detect the formation of the desired 2-thio analogue of the (6−4) photoproduct by HPLC analysis (data not shown). Therefore, in this study, we used another modified (6−4) photoproduct, $T(6-4)T^{NH2}$, in which the C2 carbonyl group of the 3′ component was replaced with an imino group. For its preparation, thymidylyl(3′−5′)-2′-deoxy-5-methylisocytidine (TpdmisoC) and oligonucleotides containing this sequence at a single site were irradiated with UV light. Prior to the UV irradiation of the oligonucleotides, photoproduct formation was confirmed using a dinucleoside monophosphate. For this purpose, a solution of TpdmisoC in 50 mM phosphate buffer (pH 7.0) was irradiated on a UV cross-linker with six 15 W germicidal lamps. The HPLC analysis revealed that the amount of TpdmisoC decreased upon UV irradiation, and a new peak, which had an absorption band with wavelengths longer than 300 nm, emerged at a retention time (t_R = 6.9 min) shorter than that of TpdmisoC (t_R = 13.9 min), in a manner similar to the formation of the (6−4) photoproduct of TpT (*18*). The UV absorption spectrum of the product extracted from the photodiode array data showed that its maximum absorption wavelength (λ_{max}) was 306 nm (Figure 2, inset). The FAB mass spectrum of this product measured in the negative ion mode revealed that its exact mass was 544.14 ([M − H]$^-$, $C_{20}H_{27}N_5O_{11}P$; calcd m/z, 544.145), although the hydrolyzed product (m/z 562.16) was also observed in the same spectrum. We measured ^{1}H NMR spectra of this product. Although the *N*-glycosidic bond of the 3′ component was completely hydrolyzed, as shown in Figure S1 of the Supporting Information, characteristic NOE signals were observed between the methyl protons of the 3′ base (δ 2.21) and H6 of the 5′ base (δ 5.02), in the same way as the (6−4) photoproduct of TpT (*18*). The chemical shift of H6 of the 3′ base (δ 8.10) demonstrated the pyrimidine-type structure of this base moiety.

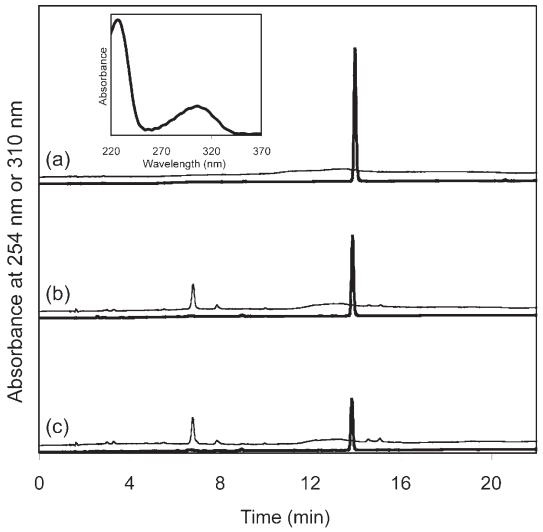

FIGURE 2: HPLC analysis after UV irradiation of thymidylyl(3′−5′)-2′-deoxy-5-methylisocytidine (TpdmisoC) for 0 (a), 20 (b), and 40 min (c). Thick and thin lines represent chromatograms monitored at 254 and 310 nm, respectively. The absorption at 310 nm was magnified by a factor of 5. The inset shows a UV absorption spectrum of the product with a t_R of 6.9 min, which was extracted with the data processing software for the photodiode array detector.

Because formation of the (6−4)-type photoproduct was confirmed, a solution of the dmisoC 12-mer, which possessed a single TpdmisoC site, was irradiated in the same way, and the reaction was analyzed by HPLC (Figure 3). A new product with the characteristic absorption at 310 nm emerged at a shorter retention time [t_R = 11.1 min (Figure 3c)], in a manner similar to that of TpdmisoC. We tried to purify the product by HPLC, but this product easily decomposed during the concentration of the TEAA-containing solution or the desalting on a gel filtration column (data not shown). Desalting using a C18 cartridge yielded a better result (Figure 3d).

The purified product was characterized by MALDI-TOF MS and nuclease digestion. In the MALDI-TOF MS analysis (Figure S2 of the Supporting Information), the obtained molecular weight was 3629.89, which was 18 units larger than the calculated

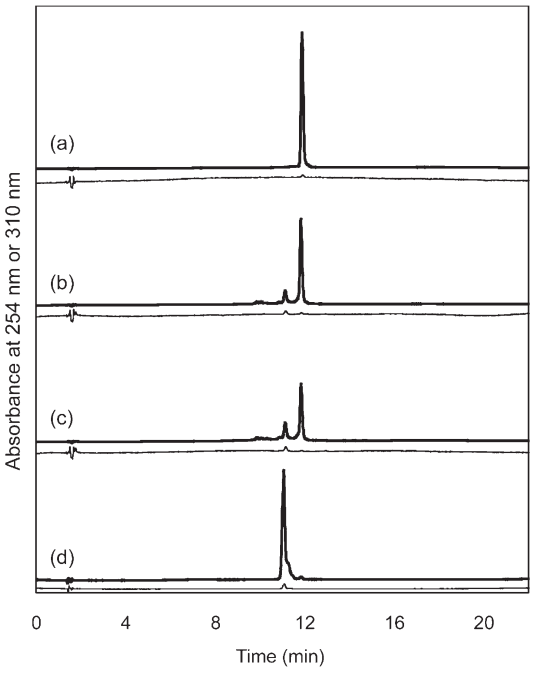

FIGURE 3: HPLC analysis of UV irradiation of the dmisoC 12-mer for 0 (a), 5 (b), and 10 min (c) and purified T(6−4)T^{NH2} 12-mer (d). Thick and thin lines represent chromatograms monitored at 254 and 310 nm, respectively. The absorption at 310 nm was magnified by a factor of 10.

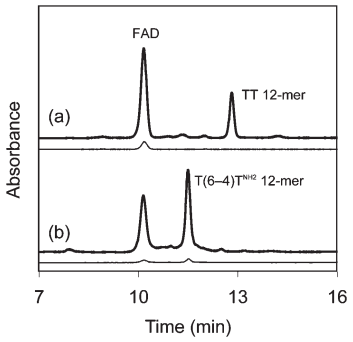

FIGURE 4: HPLC analysis of the photoreactivation of T(6−4)T 12-mer (a) and T(6−4)T^{NH2} 12-mer (b) by *Xenopus* (6−4) photolyase. Thick and thin lines represent chromatograms monitored at 254 nm and 325 (a) or 310 (b) nm, respectively. The absorption at 310 and 325 nm was magnified by a factor of 5.

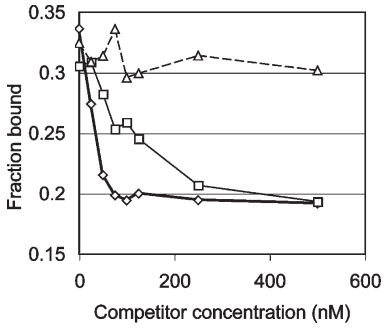

FIGURE 5: Binding of the (6−4) photolyase, as determined by a competitive EMSA. Unlabeled 15 bp duplexes containing T(6−4)T (thick line, ◇), T(6−4)T^{NH2} (thin line, □), and undamaged TT (dashed line, △) competed for (6−4) photolyase binding with [^{32}P]T(6−4)T 15 bp.

one (*m*/*z* 3612), suggesting that the product was hydrolyzed during the analysis, probably because of the acidity of the matrix. For further characterization, the product was digested with nucleases. Oligonucleotides were treated with S1 nuclease and alkaline phosphatase, as described previously (*15*), and the reaction mixtures were analyzed by HPLC (Figure S3 of the Supporting Information). The single thymidine in the dmisoC 12-mer sequence disappeared upon UV irradiation, and instead, a new peak emerged at a retention time longer than those of the four nucleosides (peak ii in trace c). This compound had two absorption maxima, at 260 and 306 nm (trace c in Figure S3B of the Supporting Information), suggesting that the 2′-deoxyadenylate on the 3′ side of T(6−4)T^{NH2} was not cleaved during the S1 nuclease digestion, in the same manner as in the T(6−4)T 12-mer digestion (trace e in Figure S3A of the Supporting Information) (*15*).

UV irradiation of the dmisoC 15-mer was performed in the same way, but in the HPLC analysis, two products, with the characteristic absorption of T(6−4)T^{NH2}, emerged at 10.2 and 12.7 min (trace d in Figure S4B of the Supporting Information). Since the product with the 10.2 min retention time was supposed to be produced by chain cleavage after the hydrolysis of the *N*-glycosidic bond, the product with the longer retention time was purified by HPLC, following the procedure for the aforementioned 12-mer, and the purified product was characterized by MALDI-TOF MS and nuclease digestion (Table S1 and Figure S3 of the Supporting Information). These analyses indicated that T(6−4)T^{NH2} was successfully formed at the TpdmisoC site in the dmisoC 15-mer.

Reaction of the (6−4) Photolyase with T(6−4)T^{NH2}. To determine whether the (6−4) photolyase can repair T(6−4)T^{NH2}, we analyzed the (6−4) photolyase reaction using the T(6−4)T^{NH2} 12-mer, by the method described previously (*15*). Although a repair assay using a restriction enzyme is available (*6*, *9*, *10*), we employed HPLC analysis because the T(6−4)T^{NH2} repair product would not be enzymatically cleaved. The T(6−4)T 12-mer and the T(6−4)T^{NH2} 12-mer were treated with *X. laevis* (6−4) photolyase under fluorescent light, and the reaction mixtures were analyzed by HPLC (Figure 4). The T(6−4)T 12-mer was converted to the undamaged oligomer (TT 12-mer) successfully (Figure 4a), and this result was confirmed by the co-injection of the reaction mixture with the TT 12-mer (data not shown). In contrast, the T(6−4)T^{NH2} 12-mer remained unrepaired (Figure 4b). The co-injection experiment assigned the peak as the starting material, i.e., the T(6−4)T^{NH2} 12-mer, and neither a prolonged reaction time (up to 23 h) nor the addition of a 10-fold molar excess of the enzyme yielded the repaired product (data not shown).

Analysis of (6−4) Photolyase Binding by an EMSA. Since the modified (6−4) photoproduct was not repaired by the (6−4) photolyase, we confirmed the binding of the (6−4) photolyase to the T(6−4)T^{NH2}-containing duplex by a competitive electrophoretic mobility shift assay (EMSA). In this experiment, the [^{32}P]T(6−4)T 15 bp duplex, ^{32}P-d(ACAGCGGT-(6−4)TGCAGGT)·d(ACCTGCAACCGCTGT), competed for (6−4) photolyase binding against increasing amounts of unlabeled 15 bp duplexes containing T(6−4)T, T(6−4)T^{NH2}, and undamaged TT. After the [^{32}P]T(6−4)T 15 bp was incubated with the (6−4) photolyase for 10 min, the competitor was added to the reaction mixture. The resultant mixture was incubated for 30 min, and then the bound and free substrates were separated by gel electrophoresis. In this experiment, a decrease in the amount of the labeled complex indicates that the competitor can bind to

the (6−4) photolyase. The fractions bound to the enzyme were plotted versus the concentration of the competitors (Figure 5). Upon the addition of T(6−4)T 15 bp, the amount of labeled complex obviously decreased and reached the lowest level at a concentration of 100 nM [Figure 5 (◇)]. For comparison, TT 15 bp, which has two thymine bases instead of the lesion, was used as a negative control, and the bound fractions were plotted similarly [Figure 5 (△)]. In this case, the addition of TT 15 bp did not cause the dissociation of the [^{32}P]T(6−4)T 15 bp−enzyme complex. In contrast, when T(6−4)T^{NH2} 15 bp was added to the solution of the [^{32}P]T(6−4)T 15 bp−enzyme complex, a smaller reduction in the amount of the bound fraction was observed [Figure 5 (□)], suggesting the (6−4) photolyase bound to T(6−4)T^{NH2} 15 bp with an affinity lower than that of T(6−4)T 15 bp.

The inhibition constant of an enzyme−competitor complex (K_i) is usually obtained from a kinetic analysis using the velocity and the Michaelis constant of the enzyme reaction in the presence of competitors (*19*). In the photolyase studies, however, the repair reaction depends on light, and the reaction is accomplished within nanoseconds (*2*, *3*). Therefore, a kinetic analysis is not appropriate for determining the K_i values of the competitors in this case. Instead, the Eadie−Scatchard plot was expanded to obtain the K_i and K_d values by formulation from the competitive inhibition scheme, as described in the Supporting Information and Figure S5. The K_d values obtained for T(6−4)T 15 bp from the experiments using T(6−4)T 15 bp and T(6−4)T^{NH2} 15 bp (106 and 110 nM, respectively) and the K_i value for T(6−4)T 15 bp (93 nM) were almost the same. The K_i value of T(6−4)T^{NH2} 15 bp (307 nM) was ∼3.3-fold lower than that of T(6−4)T 15 bp.

DISCUSSION

We intended to investigate the repair mechanisms of the (6−4) photolyase by using a (6−4) photoproduct analogue modified at the C2 carbonyl group of the 3′ pyrimidone. Thus far, two repair mechanisms for the (6−4) photolyase have been proposed. One includes hydrogen bonding interactions between the two conserved histidine side chains and the (6−4) photoproduct to form an oxetane intermediate (Figure 1A). This oxetane intermediate mechanism was derived from our experimental results that showed that the mutation of either histidine led to the loss of the repair function (*7*). The second mechanism, proposed in a structural study (*14*), hypothesizes radical formation and direct transfer of the hydroxyl group (Figure 1B). In this study, we began with the hypothesis that the UV-damaged base is repaired by the (6−4) photolyase in a manner similar to that of the CPD photolyase (*20*), by the opening of the four-membered ring. A concern with the direct transfer mechanism was that the demonstrated repair of the (6−4) photoproduct formed at the TC site (*9*, *21*) should not be achieved by direct transfer because the TC amino group is not a hydrogen-bond acceptor. A concern with the oxetane intermediate mechanism (Figure 1A) is that the N3 atom of the 3′ pyrimidone ring originally chosen as the hydrogen-bond acceptor was too close to the hydroxyl group at C5 of the 5′ component, such that the two histidine imidazole rings must be stacked to simultaneously form the two hydrogen bonds. However, such a stacking conformation was not observed in the crystal structure (*14*). Therefore, in this study, we investigated the possibility that the C2 carbonyl group of the 3′ pyrimidone functions as the hydrogen-bond acceptor.

We prepared T(6−4)T^{NH2} [**2** (Figure 1C)]. The compound 1,2-dihydro-2-imino-1-methylpyrimidine, which resembles the 3′ base of T(6−4)T^{NH2}, has a reported absorption maximum at 345 nm at pH 13. Importantly, in neutral solutions, this 2-iminopyrimidine derivative is protonated and tautomerized to an amino structure with the absorption maximum shifted to 301 nm (*22*). Therefore, if the desired T(6−4)T^{NH2} was formed by UV irradiation, then the product would be expected to have an absorption maximum at a wavelength longer than 300 nm. In fact, HPLC analysis of the UV-irradiated TpdmisoC (Figure 2) revealed the formation of a new product with an absorption maximum at 306 nm. This indicated that cationic T(6−4)T^{NH2} was successfully formed by the intramolecular Paterno−Büchi reaction and the following spontaneous oxetane splitting, similar to the formation of the (6−4) photoproduct of TpT (*18*, *23*). However, as observed in the FAB MS and NMR analyses, this product was extremely unstable even under neutral conditions, probably because of the electron deficiency of the cationic base, which induces the hydrolysis of the *N*-glycosidic bond (Scheme S1 of the Supporting Information) (*24*). This instability supports the cationic structure of the 2-aminopyrimidinium photoproduct. Although an *N*-methyl derivative of the (6−4) photoproduct, which also had a cationic 3′ base, was reportedly converted to the original pyrimidine bases by UV irradiation (*12*), we confirmed that such a photoreversion did not occur in the case of T(6−4)T^{NH2} (data not shown).

For the application to the (6−4) photolyase studies, oligonucleotides containing a single TpdmisoC were exposed to UV light, to convert the TpdmisoC site into T(6−4)T^{NH2}. We prepared two oligonucleotides containing TpdmisoC, d(CATmisoCAGCACGAC) and d(ACAGCGGTmisoCGCAGGT). This 12-mer sequence, designed in previous work (*17*), is advantageous because its repair product can be separated completely from the (6−4) photoproduct-containing oligonucleotide by reversed-phase HPLC (*15*). However, this 12-mer was not suitable for the binding experiment, because DNase I footprinting revealed that the (6−4) photolyase covers a region more than ∼10 nucleotides long around the (6−4) photoproduct (*9*, *10*). Therefore, the 15-mer was prepared for the binding assay.

In the preparation of the photoproduct, UV irradiation of the dmisoC-containing oligonucleotides yielded new products with the characteristic absorption at 310 nm, similar to the TpdmisoC case. However, MALDI-TOF MS revealed that these products were easily hydrolyzed (Table S1 of the Supporting Information). It is important to determine when the obtained products were hydrolyzed. Treatment of the oligonucleotides with S1 nuclease and alkaline phosphatase produced trimers in which an extra nucleotide remained on the 3′ side of T(6−4)T^{NH2}, as also observed for the T(6−4)T 12-mer (*15*) (traces b and e in Figure S3A of the Supporting Information). In general, after the *N*-glycosidic bond is hydrolyzed in oligonucleotides, chain cleavage by β-elimination occurs at the resultant apurinic/apyrimidinic site, as shown in Scheme S1 of the Supporting Information (*25*). Since alkaline conditions were used for the phosphatase reaction, the result described above showed that the *N*-glycosidic bond at the 3′ base of T(6−4)T^{NH2} was intact in the oligonucleotide and suggested that the hydrolysis occurred during the MALDI-TOF measurement, due to the acidity of the 3-HPA.

These oligonucleotides were used for the analysis of the (6−4) photolyase reaction. The (6−4) photolyase can convert the (6−4) photoproducts formed at TT (*6*−*10*) and TC (*9*, *21*) sites to their original bases but cannot repair the Dewar (*9*, *10*, *15*) or thietane-type photoproducts (*9*). Since the chemical structures of the latter photoproducts differ greatly from that of the (6−4) photoproduct (*26*, *27*), the (6−4) photolyase may not recognize these

photoproducts properly. In contrast, T(6−4)T^{NH2} differs from T(6−4)T at only a single functional group. Therefore, analysis of the (6−4) photolyase reaction using this modified substrate will provide useful information about the role of the functional group at this position. HPLC analysis of the (6−4) photolyase reaction revealed that T(6−4)T^{NH2} was not repaired to the original bases by the (6−4) photolyase, even in the presence of a 10-fold molar excess of the enzyme. The competitive EMSA indicated that T(6−4)T^{NH2} 15 bp clearly competed for (6−4) photolyase binding with [^{32}P]T(6−4)T 15 bp even at low concentrations, whereas the competitive binding of TT 15 bp was observed only at high concentrations, probably due to nonspecific binding. The inhibition constants of the competitors were obtained from linear approximation, as shown in Figure S5 of the Supporting Information. It should be noted that the K_d and K_i values obtained for T(6−4)T 15 bp from the experiment using T(6−4)T 15 bp (106 and 93 nM, respectively) were similar. This result indicated that this method could be used to analyze the enzyme binding, because these parameters, which both showed the affinity for T(6−4)T, should be the same. By using this plot, a K_i value of 307 nM was obtained for T(6−4)T^{NH2} 15 bp, which was 3.3-fold lower than that for T(6−4)T 15 bp. These results demonstrate that the (6−4) photolyase could bind to T(6−4)T^{NH2}, although the affinity was reduced to some extent, as compared to that for T(6−4)T.

Our study revealed that T(6−4)T^{NH2} bound to the (6−4) photolyase with considerable affinity but was not repaired. These results indicate that the C2 carbonyl group in the 3′ pyrimidone of the (6−4) photoproduct plays a role in the enzymatic repair mechanism. Two repair mechanisms have been proposed, as shown in Figure 1. In the direct transfer mechanism (Figure 1B), the substitution of the carbonyl group with the iminium group in the 3′ base of the (6−4) photoproduct may facilitate the nucleophilic attack of the water molecule at C4 of the 3′ base and does not affect the following (6−4) bond cleavage. On the other hand, the results obtained in this study can be explained by the oxetane-mediated mechanism. The modification we introduced in this study was the replacement of the C2 carbonyl group in T(6−4)T with an iminium group, and the primary difference between these two groups is their role in hydrogen-bond formation. The carbonyl and iminium groups work as an acceptor and a donor, respectively. Therefore, our results suggested that the functional group at this position is involved in a hydrogen bonding interaction with the enzyme. Considering the results of our (6−4) photolyase reaction and the oxetane intermediate mechanism, we propose that the second hydrogen bond is formed between the carbonyl group and an amino acid residue of the enzyme (Figure 6). An acidic side chain (HA, in Figure 6) would interact with the C2 carbonyl group, not N3, in the 3′ pyrimidone of the (6−4) photoproduct, while the C5 hydroxyl group in the 5′ component forms a hydrogen bond with a basic residue (B:). These residues may be the conserved histidine side chains. The hydroxyl group attacks C4 of the 3′ pyrimidone to form the oxetane intermediate in a concerted manner, as shown in Figure 6. Subsequently, the (6−4) photoproduct is repaired by transfer of an electron from the excited FADH$^-$.

In conclusion, we prepared and characterized the modified (6−4) photoproduct, T(6−4)T^{NH2}, in which the carbonyl group was replaced with an imine, to analyze the (6−4) photolyase reaction. We found that T(6−4)T^{NH2} is not repaired to the original bases, although the enzyme binds to this substrate analogue with considerable affinity, indicating that the C2 carbonyl group of the (6−4) photoproduct plays an important role in the (6−4) photolyase reaction. This finding will contribute to the elucidation of the recognition and reaction mechanisms of the (6−4) photolyase.

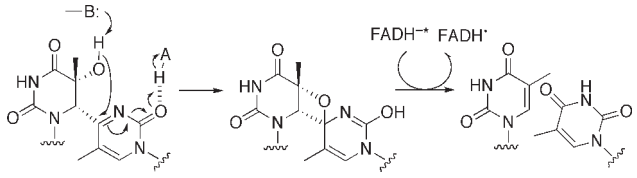

FIGURE 6: Revised mechanism of the (6−4) photolyase reaction, using the C2 carbonyl group as a hydrogen-bond acceptor.

SUPPORTING INFORMATION AVAILABLE

Summary of the MALDI-TOF MS results (Table S1), NMR spectrum of T(6−4)T^{NH2} (Figure S1), MALDI-TOF mass spectrum of the T(6−4)T^{NH2} 12-mer (Figure S2), HPLC analysis of nuclease digestions of the oligonucleotides used in this study (Figure S3), HPLC chromatograms of UV irradiation of TT 15-mer and dmisoC 15-mer (Figure S4), and the expanded Eadie−Scatchard plot (Figure S5 and Supplementary methods). This material is available free of charge via the Internet at http://pubs.acs.org.

REFERENCES

1. Iwai, S. (2008) Pyrimidine Dimers: UV-induced DNA Damage. In Modified Nucleosides in Biochemistry, Biotechnology and Medicine (Herdewijn, P., Ed.) Chapter 5, pp 97−131, Wiley-VCH, Weinheim, Germany.
2. Sancar, A. (2003) Structure and function of DNA photolyase and cryptochrome blue-light photoreceptors. *Chem. Rev. 103*, 2203–2237.
3. Weber, S. (2005) Light-driven enzymatic catalysis of DNA repair: A review of recent biophysical studies on photolyase. *Biochim. Biophys. Acta 1707*, 1–23.
4. Mees, A., Klar, T., Gnau, P., Hennecke, U., Eker, A. P. M., Carell, T., and Essen, L.-O. (2004) Crystal structure of a photolyase bound to a CPD-like DNA lesion after in situ repair. *Science 306*, 1789–1793.
5. Sancar, A. (2008) Structure and function of photolyase and in vivo enzymology: 50th anniversary. *J. Biol. Chem. 283*, 32153–32157.
6. Kim, S.-T., Malhotra, K., Smith, C. A., Taylor, J.-S., and Sancar, A. (1994) Characterization of (6−4) photoproduct DNA photolyase. *J. Biol. Chem. 269*, 8535–8540.
7. Hitomi, K., Nakamura, H., Kim, S.-T., Mizukoshi, T., Ishikawa, T., Iwai, S., and Todo, T. (2001) Role of two histidines in the (6−4) photolyase reaction. *J. Biol. Chem. 276*, 10103–10109.
8. Schleicher, E., Hitomi, K., Kay, C. W. M., Getzoff, E. D., Todo, T., and Weber, S. (2007) Electron nuclear double resonance differentiates complementary roles for active site histidines in (6−4) photolyase. *J. Biol. Chem. 282*, 4738–4747.
9. Zhao, X., Liu, J., Hsu, D. S., Zhao, S., Taylor, J.-S., and Sancar, A. (1997) Reaction mechanism of (6−4) photolyase. *J. Biol. Chem. 272*, 32580–32590.
10. Hitomi, K., Kim, S.-T., Iwai, S., Harima, N., Otoshi, E., Ikenaga, M., and Todo, T. (1997) Binding and catalytic properties of *Xenopus* (6−4) photolyase. *J. Biol. Chem. 272*, 32591–32598.
11. Cichon, M. K., Arnold, S., and Carell, T. (2002) A (6−4) photolyase model: Repair of DNA (6−4) lesions requires a reduced and deprotonated flavin. *Angew. Chem., Int. Ed. 41*, 767–770.
12. Asgatay, S., Petermann, C., Harakat, D., Guillaume, D., Taylor, J.-S., and Clivio, P. (2008) Evidence that the (6−4) photolyase mechanism can proceed through an oxetane intermediate. *J. Am. Chem. Soc. 130*, 12618–12619.
13. Borg, O. A., Eriksson, L. A., and Durbeej, B. (2007) Electron-transfer induced repair of 6−4 photoproducts in DNA: A computational study. *J. Phys. Chem. A 111*, 2351–2361.
14. Maul, M. J., Barends, T. R., Glas, A. F., Cryle, M. J., Domratcheva, T., Schneider, S., Schlichting, I., and Carell, T. (2008) Crystal structure and mechanism of a DNA (6−4) photolyase. *Angew. Chem., Int. Ed. 47*, 10076–10080.
15. Yamamoto, J., Hitomi, K., Todo, T., and Iwai, S. (2006) Chemical synthesis of oligodeoxyribonucleotides containing the Dewar valence

isomer of the (6−4) photoproduct and their use in (6−4) photolyase studies. *Nucleic Acids Res. 34*, 4406–4415.
16. Yamamoto, J., Tanaka, Y., and Iwai, S. (2009) Spectroscopic analysis of the pyrimidine(6−4)pyrimidone photoproduct: Insights into the (6−4) photolyase reaction. *Org. Biomol. Chem. 7*, 161–166.
17. Fujiwara, Y., and Iwai, S. (1997) Thermodynamic studies of the hybridization properties of photolesions in DNA. *Biochemistry 36*, 1544–1550.
18. Rycyna, R. E., and Alderfer, J. L. (1985) UV irradiation of nucleic acids: Formation, purification and solution conformational analysis of the '6−4 lesion' of dTpdT. *Nucleic Acids Res. 13*, 5949–5963.
19. Fersht, A. (1998) The basic equations of enzyme kinetics. In Structure and mechanism in protein science: A guide to enzyme catalysis and protein folding (Hadler, G. L., Ed.) 4th ed., Chapter 3, pp 103−131, Freeman, New York.
20. Todo, T., Ryo, H., Yamamoto, K., Toh, H., Inui, T., Ayaki, H., Nomura, T., and Ikenaga, M. (1996) Similarity among the *Drosophila* (6−4) photolyase, a human photolyase homolog, and the DNA photolyase-blue-light photoreceptor family. *Science 272*, 109–112.
21. Mizukoshi, T., Hitomi, K., Todo, T., and Iwai, S. (1998) Studies on the chemical synthesis of oligonucleotides containing the (6−4) photoproduct of thymine-cytosine and its repair by (6−4) photolyase. *J. Am. Chem. Soc. 120*, 10634–10642.
22. Brown, D. J., Hoerger, E., and Mason, S. F. (1955) Simple pyrimidines. Part III. The methylation and structure of the aminopyrimidines. *J. Chem. Soc.*, 4035–4040.
23. Rahn, R. O., and Hosszu, J. L. (1969) Photochemical studies of thymine in ice. *Photochem. Photobiol. 10*, 131–137.
24. Rios-Font, R., Rodriguez-Santiago, L., Bertran, J., and Sudupe, M. (2007) Influence of N7 protonation on the mechanism of the N-glycosidic bond hydrolysis in 2′-deoxyguanosine. A theoretical study. *J. Phys. Chem. B 111*, 6071–6077.
25. Lhomme, J., Constant, J.-F., and Demeunynck, M. (1999) Abasic DNA structure, reactivity, and recognition. *Biopolymers 52*, 65–83.
26. Taylor, J.-S., Garrett, D. S., and Cohrs, M. P. (1988) Solution-state structure of the Dewar pyrimidinone photoproduct of thymidylyl-(3′→5′)-thymidine. *Biochemistry 27*, 7206–7215.
27. Clivio, P., Fourrey, J.-L., and Gasche, J. (1991) DNA photodamage mechanistic studies: Characterization of a thietane intermediate in a model reaction relevant to "6−4 lesions". *J. Am. Chem. Soc. 113*, 5481–5483.